Comparison of Flux Control Capability of a Series Double Excitation Machine and a Parallel Double Excitation Machine

Y. Amara[1], G. Barakat[1] and M. Gabsi[2]
[1]GREAH, EA 3220, Université du Havre, 76063 Le Havre, France
[2]SATIE, UMR 8029, Ecole Normale Supérieure de Cachan, 94230 Cachan, France
E-mail: yacine.amara@univ-lehavre.fr

***Abstract*-This paper presents a comparison of open circuit flux control capability of two structures of double excitation synchronous machines. First, the structures of these two machines are presented: one is a series double excitation machine and the other one is a parallel double excitation machine. The flux control capability of the parallel double excitation machine is evaluated experimentally using a build prototype. For the study of flux control capability of the series double excitation machine, a 2D exact analytical solution of open circuit magnetic field distribution in a idealized geometry of a series double excitation synchronous machine is established. It involves solution of Maxwell's equations in stator slots, airgap, PM's region and rotor slots. The validity of developed model is demonstrated via comparison to finite element analyses. Then, developed model is used to study the open circuit flux control of a series double excitation machine having same overall dimensions as the parallel double excitation machine prototype. Finally, open circuit flux control capabilities of both structures are compared.**

I. INTRODUCTION

This paper presents a comparison of open circuit flux control capability of two structures of double excitation synchronous machines. Double excitation machines are synchronous machines where two excitation field sources coexist [1] [2]: permanent magnets and wound field excitation. The goal behind the principle of double excitation is to combine advantages of PM excited machines and wound field synchronous machines. This kind of machines can constitute good candidate for electric or hybrid vehicles traction [3], [4]. The flux control capability of the parallel double excitation machine is evaluated experimentally using a build prototype.

For the study of flux control capability of the series double excitation machine, a 2D exact analytical solution of open circuit magnetic field distribution in an idealized geometry of a series double excitation synchronous machine is established. The developed model gives exact field distribution due to permanent magnet and excitation coils in the stator slots region, the airgap region, the PM's region and the rotor slots. Analytical solutions for the field in double excitation machines, which would be extremely useful for their design and performance optimization, have not been available in literature, to date. The slotted stator has a classical configuration with radial teeth. The slots and teeth can be equally distributed or not [5], [6]. They can be arranged to accommodate any winding configuration (overlapping and non overlapping windings). The validity of developed model is demonstrated via comparison to finite element analyses. The developed model is then used to study the open circuit flux control of a series double excitation machine having same overall dimensions as the parallel double excitation machine prototype. Finally, open circuit flux control capabilities of both structures are compared.

II. DOUBLE EXCITATION MACHINES

Figures 1(a) and 1(b) shows respectively the stator and rotor of a 3 kW prototype of parallel double excitation machine. Figure 1(c) shows the structure of the series double excitation synchronous machine [2]. Table I gives the parallel double excitation synchronous machine main data. Figure 2 shows a 3D cut view of the parallel double excitation machine.

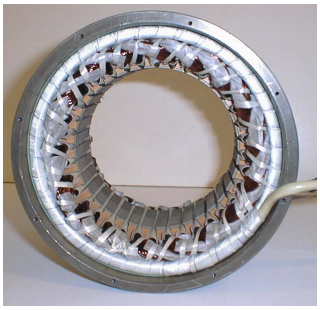

(a) Stator of parallel double excitation machine

(b) Rotor of parallel double excitation machine

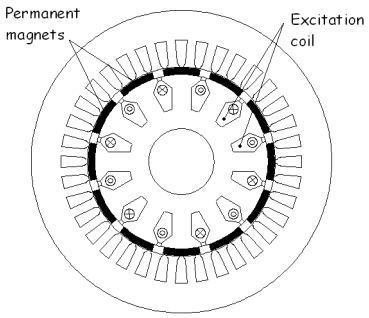

(c) Series double excitation machine

Fig. 1. Double excitation machines.

978-1-4244-8218-4/10/$26.00 ©2010 IEEE

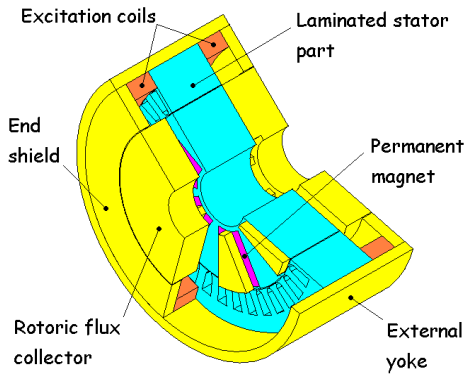

Fig. 2. 3D cut view of the parallel double excitation machine.

TABLE I
PARALLEL DOUBLE EXCITATION SYNCHRONOUS MACHINE DATA

Stator outer diameter (mm)	184
Stator inner diameter (mm)	115
Air gap thickness (mm)	0.5
Machine's axial length (mm)	115
Active part length (mm)	40
Number of poles	12
Number of phases	3
Magnet type	Ferrite
Magnet dimensions (thickness, height, length) (mm)	(6, 40, 44)

Open circuit flux control principle is described in following subsections.

A. Parallel hybrid excitation machine operating principle

Figure 3 shows principle trajectory of flux created by permanent magnets. This flux circulates from one pole to another as for classical permanent magnet machines using flux focusing principle.

Figure 4 shows wound field excitation flux trajectories. The machine has two annular excitation coils. Each coil is acting in one kind of magnetic poles. The flux created by an excitation coil passes one time through active part's airgap (homoplar path). Depending on DC excitation current direction, excitation coils can either be used to enhance or decrease (weaken) excitation flux passing through armature windings. More details about operation of this structure can be found in [3].

B. Series hybrid excitation machine operating principle

Figure 5 illustrates the open circuit airgap flux control principle for the series double excitation machine.

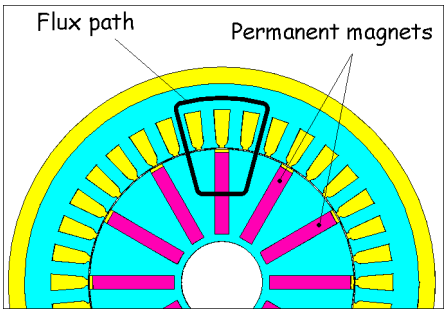

Fig. 3. PM excitation flux trajectory.

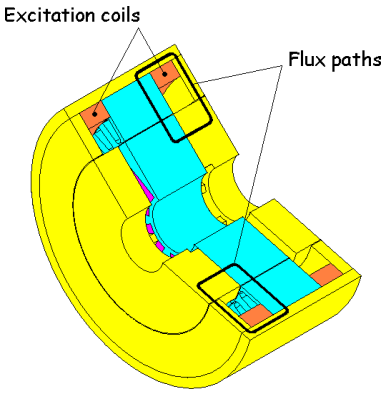

Fig. 4. Wound field excitation flux trajectories.

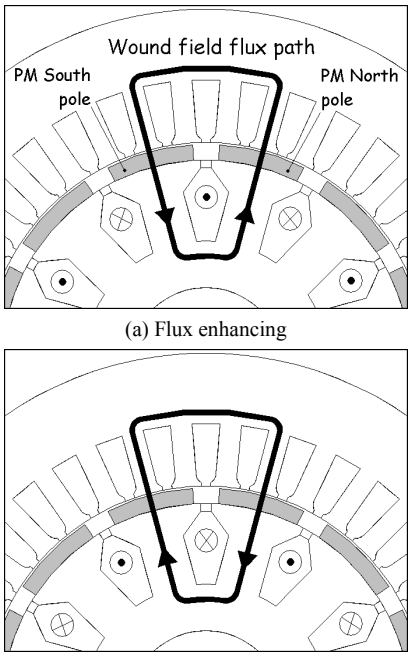

(a) Flux enhancing

(b) Flux weakening

Fig. 5. Open circuit flux control principle of series double excitation machine.

Depending on DC excitation current direction, excitation coils can either be used to enhance (Fig. 5(a)) or decrease (weaken) (Fig. 5(b)) excitation flux passing through armature windings. More details about operation of this structure can be found in [2].

III. OPEN CIRCUIT MAGNETIC FIELD SOLUTION OF SERIES DOUBLE EXCITATION MACHINE

Figure 6 shows the different regions (stator slots (I), airgap (II), permanent magnets (III), rotor slots (IV)) where the exact analytical solution is established thanks to separation of variables method. The model is formulated in two-dimensional polar coordinates. The analytical solution for the magnetic field distribution is established based on following assumptions: 1) the stator and rotor cores are assumed to be infinitely permeable. However, main magnetic saturation can be accounted in an iterative way by adapting the geometrical length of the airgap [7] [8]; 2) eddy current effects are

neglected (no eddy current loss in the magnets or armature windings); 3) the permeability of permanent magnets is assumed to be equal to that of air; and finally, 4) the axial length of the machines is infinite so that the end effects are neglected. However, fringing effects associated with the finite length can be taken into account [9].

Figure 6 shows the idealized series double excitation machine geometry with principal dimensions and the different field regions. θ_r and θ_s represent respectively the pole pitch and the slot pitch. In order to simplify the understanding of the mathematical approach only equally distributed slots topologies are considered in this study. However unequally distributed slots topologies [5] [6] can also be modelised using exactly the same mathematical approach [5].

The partial differential equation for quasi-stationary magnetic fields in a continuous and isotropic region can be expressed in terms of the magnetic vector potential **A**, subject to the Coulomb gauge, $\nabla \times \mathbf{A} = 0$, by

$$\begin{cases} \nabla^2 \mathbf{A} = 0, & \text{in regions I and II} \\ \nabla^2 \mathbf{A} = -\mu_0 \nabla \times \mathbf{M}, & \text{in region III} \\ \nabla^2 \mathbf{A} = -\mu_0 \mathbf{J}_\mathrm{f}, & \text{in regions IV} \end{cases} \quad (1)$$

A only has A_z component which is independent of z (infinitely long machine in axial direction). **M** is the magnetization and $\mathbf{J}_\mathrm{f}$ is the DC field current density.

The field vectors **B** and **H**, in the different regions, are coupled by

$$\mathbf{B} = \begin{cases} \mu_0 \mathbf{H}, & \text{in regions I, II and IV} \\ \mu_0 (\mathbf{H} + \mathbf{M}), & \text{in region III} \end{cases} \quad (2)$$

where magnetic field vector **B** components are deduced from A_z by

$$B_r = \frac{1}{r}\frac{\partial A_z}{\partial \varphi} \; ; \; B_\varphi = -\frac{\partial A_z}{\partial r} \quad (3)$$

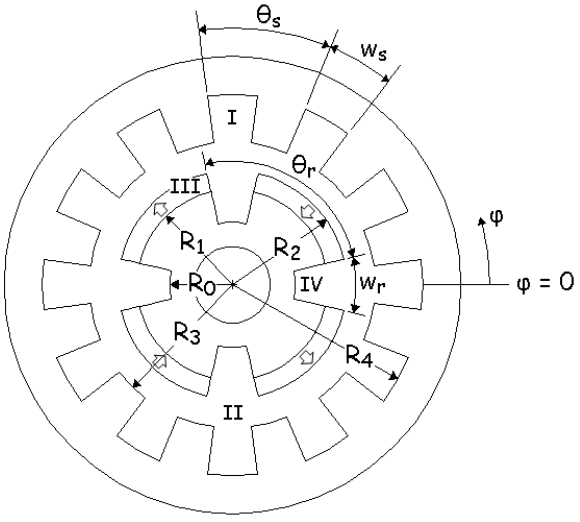

Fig. 6. Idealized series double excitation synchronous machine.

and remanent magnetization vector **M** components can be expressed as follows:

$$\begin{cases} M_r = \sum_{n=1}^{+\infty} \left(M_{r1n} \cos(m_n \varphi) + M_{r2n} \sin(m_n \varphi) \right) \\ M_\varphi = \sum_{n=1}^{+\infty} \left(M_{\varphi 1n} \cos(m_n \varphi) + M_{\varphi 2n} \sin(m_n \varphi) \right) \end{cases} \quad (4)$$

with $m_n = n \times \lambda$, where $\lambda = \gcd(N_s, p)$, with N_s being the number of slots and p the number of pole pairs.

Since the stator and rotor cores are assumed to be infinitely permeable the analysis is reduced to a linear problem, and the open circuit magnetic field distribution for a given excitation current is obtained by the superposition of magnetic field due to permanent magnets and magnetic field due to excitation current.

Equation (1) can be rewritten in polar coordinates as

$$\frac{1}{r}\frac{\partial}{\partial r}\left(r \frac{\partial A_z}{\partial r} \right) + \frac{1}{r^2}\frac{\partial^2 A_z}{\partial \varphi^2} = \begin{cases} 0 & \text{in regions I and II} \\ -\mu_0 \nabla \times \mathbf{M} & \text{in region III} \\ -\mu_0 \mathbf{J}_\mathrm{f} & \text{in region IV} \end{cases} \quad (5)$$

The general solution of equation (5) is obtained thanks to separation of variables method and can be written as follows:

$$A_z = a_0 + A_{ps}(r, \varphi) + \sum_{n=1}^{+\infty} \begin{bmatrix} \left(a_{1n} r^{m_n} + a_{2n} r^{-m_n} \right) \cos(m_n \varphi) \\ + \left(a_{3n} r^{m_n} + a_{4n} r^{-m_n} \right) \sin(m_n \varphi) \end{bmatrix} \quad (6)$$

A_{ps} is the particular solution of equation (5) for only the permanent magnets region and rotor slots region (regions III and IV).

For machines with $\lambda = 1$, particular solution in region III is given by:

$$A_{ps} = \begin{pmatrix} r \sum_{n=2}^{+\infty} \left[a_{5n} \cos(m_n \varphi) + a_{6n} \sin(m_n \varphi) \right] \\ + \begin{bmatrix} \left(a_{11} r + a_{21} r^{-1} + a_{51} r \, \mathrm{Ln}(r) \right) \cos(\varphi) \\ + \left(a_{31} r + a_{41} r^{-1} + a_{61} r \, \mathrm{Ln}(r) \right) \sin(\varphi) \end{bmatrix} \end{pmatrix} \quad (7)$$

while for machines with $\lambda > 1$, particular solution in this region is given by:

$$A_{ps} = r \sum_{n=1}^{+\infty} \left[a_{5n} \cos(m_n \varphi) + a_{6n} \sin(m_n \varphi) \right] \quad (8)$$

Particular solution for regions IV (rotor slots) is given, in a rotor slot '*j*', by

$$A_{ps} = -\frac{\mu_0}{2} J_f^{(j)} \left(R_0^2 \, \mathrm{Ln}(r) - \frac{r^2}{2} \right) \quad (9)$$

Combining solutions of magnetic field components, obtained from equations (3) and (6), with boundary conditions in each region helps to establish a set of linear equations (N_H x N_H) (where N_H is the number of considered harmonics), where coefficients of magnetic vector potential

solution in region III are the unknown. Solving these linear equations and using interface conditions give coefficients of magnetic vector potential in other regions. Obtained linear system is solved using Gaussian elimination method. The developed model takes into account rotor movement.

Table II gives some characteristics of the machine to which both methods (analytical technique and finite element) have been applied. Finite element method has been applied to real geometry of machine with a relative permeability of 1e6 for stator and rotor cores. The finite element solutions were obtained using the model shown in Fig. 7 by applying a periodic boundary condition at the angular boundaries $\varphi = 0$ and $\varphi = 2\pi/3$ and imposing the natural Dirichlet boundary condition at the other bounding surface (inner and outer structure radii).

Figure 8 compares analytically predicted and finite-element-calculated open-circuit distributions of magnetic field components, due to permanent magnet and excitation current (J_f = 5 A/mm^2), as functions of the angular position in the different machine's regions. Excitation coils are fed such as created flux is opposing excitation flux created by permanent magnets. As can be seen the analytical predictions agree well with the finite-element computations.

IV. Comparison of Open Circuit Flux Control Capability

Figure 9 compares variations of maximum air gap flux per unit length versus field MMF of the parallel double excitation synchronous machine (PDESM) and three different series double excitation synchronous machines (SDESM). Table III gives series double excitation synchronous machines main parameters. It can be seen that a wide range of air gap flux control can be achieved for the parallel double excitation machine. The air-gap flux changes with a variation of +95%, when air gap flux is enhanced, and –70%, when it is weakened, with respect to the no-field excitation flux.

TABLE II – Machines Parameters

Poles number	6
Slot number	18
Magnets distribution	Radial
Magnet type	NdFeB (residual induction = 1T)
R_0, R_1, R_2, R_3 and R_4 (mm)	26.67, 50, 56, 57.5 and 81.5
ws (rad)	π / 18
wr (rad)	π / 15

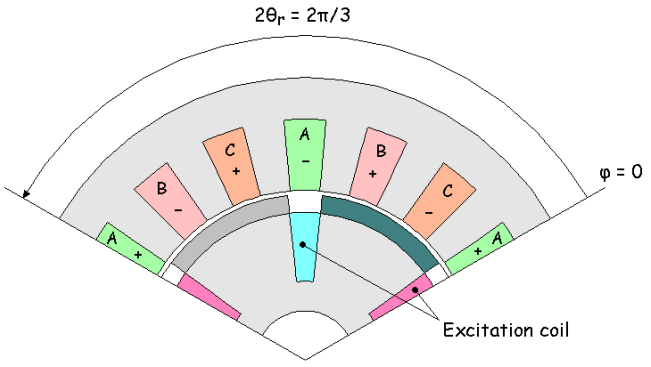

Fig. 7. Finite element model.

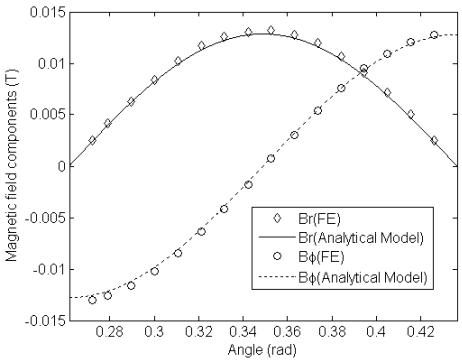

(a) ($r = (R_3+R_4) / 2$, region I (stator slots))

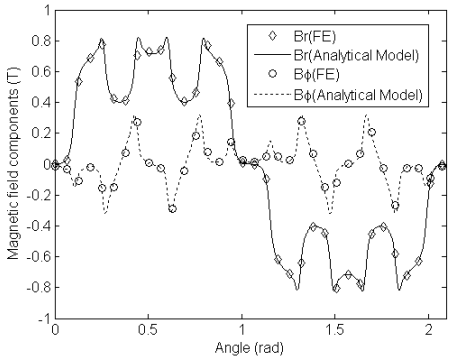

(b) ($r = (R_2+R_3) / 2$, region II (airgap))

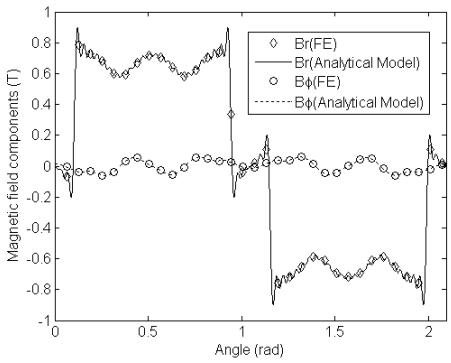

(c) ($r = (R_1+R_2) / 2$, region III (permanent magnet))

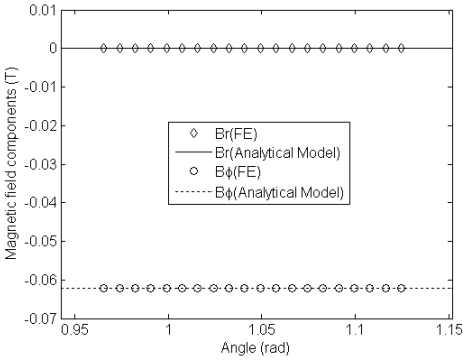

(d) ($r = (R_0+R_1) / 2$, region IV (rotor slots))

Fig. 8. Comparison of magnetic field space distribution by both finite element and analytical model (magnetic field due to permanent magnets).

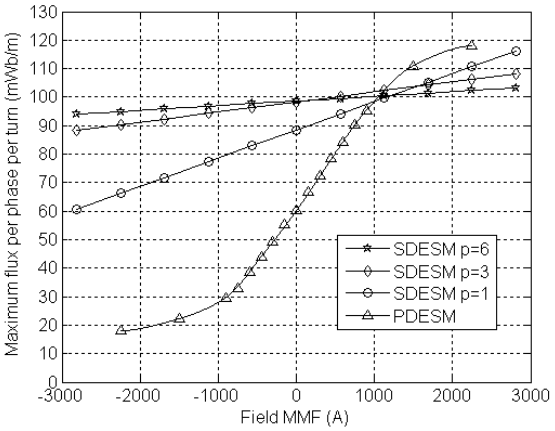

Fig. 9. Comparison of open circuit flux control capability.

TABLE III – SERIES DOUBLE EXCITATION MACHINES PARAMETERS

Poles number	p = 1, 3 or 6
Slot number	6×p
Magnets distribution	Radial
Magnet type	NdFeB (residual induction = 1T)
R_1 (mm)	26.67
R_1 (mm)	50
R_2 (mm)	56
R_3 (mm)	57.5
R_4 (mm)	81.5
ws (rad)	π / (6p)
wr (rad)	π / (5p)

The airgap thickness of series double excitation machines is chosen to be equal to 1.5 mm to allow for a permanent magnets containment system (thin sleeve, adhesive impregnated glass tape, carbon fiber, or other high strength fiber banding) [10].

The three series double excitation machines have different number of pole pairs, respectively 1, 3 and 6. The series double excitation machine with one pole pair (p = 1) has better performance in term of flux control compared to other series double excitation machines. However, since the number of pole pairs is the lowest, the power density of this machine is lower than two others series double excitation machines. End windings length should be longer for this machine compared to others machines.

The improvement of open circuit flux control capability of the one pole pair series double excitation machine is due to the fact that magnetic reluctance seen by excitation coils reduces when the number of poles pairs decreases. Table IV gives the maximum value of magnetic mutual permeance between an armature phase and excitation coils for the different series double excitation machines. As can be seen this mutual is the higher for the one pole pair machine. However, even thought that flux control capability of this machines (SDESM with p = 1) is better than two others series double excitation machines (p =3 and 6), it is still lower than that of the parallel double excitation synchronous machines. Furthermore, it should be noticed that for series double excitation machines the risk of partial irreversible demagnetization increases when the flux control capability is improved.

TABLE IV – MUTUAL PERMEANCES

Poles number	Mutual permeance maximum value (μH/m)
2 (p = 1)	10
6 (p = 3)	3.54
12 (p = 6)	1.63

Figure 10 shows lower value of flux density radial component distribution map in a permanent magnet for the one pole pair machine when the field MMF is equal to – 1686 A (J_f = 3 A/mm^2).

If we consider that the NdFeB magnets used in series double excitation machine are of Neomag S35UC grade and that the operating temperature of the machine can reach 180°C, irreversible demagnetization will occur if the flux density reduces to less than 0.3 T in the direction of magnetisation [11]. As can be observed there are regions in the magnets, in particular at the surface of magnets, in which the flux density in the direction of magnetization falls below the 0.3 T. Thus, these regions will be irreversibly demagnetized if the magnets operating temperature reaches 180°C. Temperature rise effect combined to the fact that excitation flux passes trough permanent magnets in series double excitation machines increases the risk of permanent magnets demagnetization when the airgap excitation flux is weakened.

For the parallel double excitation machine since ferrite magnets are used, the loss of performance will be important if the temperature reaches 180°C. However, it should be noticed that ferrite magnets can be easily replaced by NdFeB magnets. The use of NdFeB magnets helps increase excitation flux due to permanent magnets which can reach the same level compared to series double excitation machines (Fig. 9). Furthermore, since excitation flux created by excitation coils does not pass trough permanent magnets in parallel double excitation machines, demagnetization risk is only increased by the temperature rise effect.

V. CONCLUSION

This paper presented a comparison study of open circuit flux control capability of a parallel double excitation machine and a series double excitation machines. The flux control capability of the parallel double excitation machine is

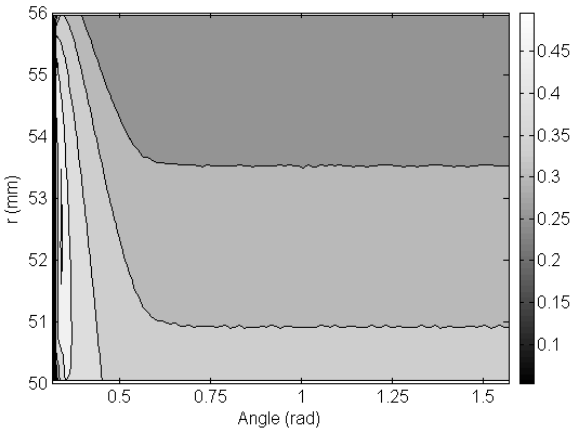

Fig. 10. Flux density lower value distribution map in a permanent magnet.

evaluated experimentally using a build prototype. For the study of flux control capability of the series double excitation machine, a 2D exact analytical solution of open circuit magnetic field distribution in an idealized geometry of a series double excitation synchronous machine is established.

This study has shown the advantages brought by the principle of parallel double excitation machines over series double excitation principle in term of open circuit flux control capability.

REFERENCES

[1] Y. Amara, J. Lucidarme, M. Gabsi, M. Lécrivain, A. H. Ben Ahmed and A. D. Akémakou, "A new topology of hybrid excitation synchronous machine," *IEEE Trans. Ind. Applications*, vol. 37, no. 5, pp. 1273-1281, September/October 2001.

[2] G. Henneberger and J.R. Hadji-Minaglou and R.C. Ciorba, "Design and test of permanent magnet synchronous motor with auxiliary excitation winding for electric vehicle application," European Power Electronics Chapter Symposium, Lausanne, October, 1994, pp. 645 – 649.J.

[3] Y. Amara, L. Vido, M. Gabsi, E. Hoang, A. H. Ben Ahmed and M. Lécrivain, "Hybrid excitation synchronous machines: energy-efficient solution for vehicles propulsion," *IEEE Trans. Vehicular Technology*, vol. 58, no. 5, pp. 2137-2149, June 2009.

[4] J.R. Hadji-Minaglou and G. Henneberger, "Comparison of different motor types for electric vehicle application," *European Power Electronics and Drives Journal* (*EPE Journal*), vol. 8, no. 3 – 4, pp. 46-55, September 1999.

[5] J. Azzouzi, G. Barakat and B. Dakyo, "Quasi-3-D analytical modeling of the magnetic field of an axial flux permanent-magnet synchronous machine," *IEEE Trans. Energy Convers.*, vol. 20, no. 4, pp. 746–752, December 2005.

[6] D. Ishak, Z. Q. Zhu and D. Howe, "Permanent-magnet brushless machines with unequal tooth widths and similar slot and pole numbers," *IEEE Trans. Ind. Applications*, vol. 41, no. 2, pp. 584-590, March/April 2005.

[7] N. Boules, "Two-dimensional field analysis of cylindrical machines with permanent magnet excitation," *IEEE Trans. Ind. Applications*, vol. 20, no. 5, pp. 1267-1277, September/October 1984.

[8] J. Wang and D. Howe, "Design optimization of radially magnetized, iron-cored, tubular permanent-magnet machines and drives systems," *IEEE Trans. Magn.*, vol. 40, no. 5, pp. 3262-3277, September 2004.

[9] G. Qishan and G. Hongzhan, "The fringing effect in PM electric machines," *Electric machines and power systems*, vol. 11, n° 2, pp. 159-169, 1986.

[10] H. A. Toliyat and G. B. Kliman, *Handbook of electric motors,* 2nd ed., Marcel Dekker, Inc., 2004.

[11] J. Wang, W. Wang, K. Atallah and D. Howe, "Demagnetization assessment for three-phase tubular brushless permanent-magnet machines," *IEEE Trans. Magn.*, vol. 44, no. 9, pp. 2195-2203, September 2008.